Journal of Applied Polymer Science

Dependence of Alcohol Vapor-Induced Crystallization on Gas and Vapor Permeabilities of Poly(lactic acid) Films

Shuichi Sato, Takayuki Wada, Ryohei Ido, Yoshiyuki Murakoshi, Shinji Kanehashi, Kazukiyo Nagai
Department of Applied Chemistry, Meiji University, Tama-ku, Kawasaki 214-8571, Japan
Correspondence to: K. Nagai (E-mail: nagai@meiji.ac.jp)

ABSTRACT: The effects of methanol and ethanol vapor-induced crystallization on vapor and gas permeabilities and on the structure of poly(lactic acid) (PLA) films were systematically investigated. At high temperature conditions, the vapor permeability of PLA films decreased with increasing exposure time. The PLA films that were exposed to alcohol vapor became slightly cloudy, and no changes in chemical structure were observed. Alcohol vapor-induced crystallization formed α-crystal structure. The vapor permeability decreased with increasing crystallinity. However, nitrogen permeability slightly increased after vapor-induced crystallization. The dependence of crystallinity on vapor and gas permeabilities was different from each penetrant. Total crystalline structures, including continuous crystal structures, remaining amorphous regions, and their interface depend on vapor and gas permeabilities. © 2013 Wiley Periodicals, Inc. J. Appl. Polym. Sci. **2014**, *131*, 40140.

KEYWORDS: biodegradable; biopolymers & renewable polymers; poly(lactic acid); solvent-induced crystallization; gas and vapor permeability

Received 29 July 2013; accepted 30 October 2013
DOI: 10.1002/app.40140

INTRODUCTION

Poly(lactic acid) (PLA) is an environmentally friendly, biodegradable polymer with a low melting point and high moldability. PLA is used as a material in packaging, automobiles, and electronics. In these applications, polymer materials are exposed to organic vapors, including alcohol vapor, during use. The permeation property of organic vapors is a very important factor in designing these materials. However, few reports are available on the transport properties of organic vapor. The sorption properties of ethyl lactate and aromatic hydrocarbon solvents were already reported, but the systematic investigation on the permeation property of alcohol vapors has not been conducted.[1,2]

Methanol- and ethanol-induced PLA crystallization has been reported in our previous study.[3] PLA is an interesting polymer whose gas permeability is not significantly affected by its isomer ratio and crystallinity.[4,5] In the L:D-donor ratio range of 98.7:1.3 to 50:50 and in the crystallinity range of 0% to 25%, the oxygen permeability coefficients of the PLA sample were between 1.7 to 3.4 $\times$ 10^{-11} cm^3(STP)cm/(cm^2 s cmHg) at 30 to 35°C. In general, gas permeability decreases with increasing polymer crystallinity. This phenomenon is attributed to the inability of gas molecules to diffuse and dissolve in the crystalline domain.[6] However, in our recent report, we found that gas transport properties are independent of PLA crystallinity.[5,7] The relationship between gas permeability and crystallinity was discussed and only the gas- (i.e., nitrogen, oxygen, and carbon dioxide) and thermally-induced crystallized PLA film was focused. Although vapor permeability shows a different behavior, no direct evidence on the relationship between alcohol vapor permeability and alcohol-induced crystallized PLA structure is currently available. This study systematically investigates the effects of alcohol-induced crystallization on the alcohol vapor permeability of PLA film and their structures.

EXPERIMENTAL

Film Preparation

We used the same PLA films as in our previous study.[3,7,8] The PLA polymer used in this study had a 4032D film (NatureWorks LLC, Minnetonka, MN), and the L:D isomer ratio ranged from 96.0:4.0 to 96.8:3.2. The weight average molecular weight, M_w, the number average molecular weight, M_n, and the molecular weight distribution ratio, M_w/M_n, of the polymer were determined using a gel permeation chromatograph (HLC-8220, Tosoh Co., Tokyo, Japan) with TSK-gel columns (Super AWM-H) and detector (RI-8220). The range of M_n, M_w, and M_w/M_n were from 67,200 to 81,100 g/mol, from 124,400 to 167,400 g/mol, and from 1.838 to 2.007, respectively.

The PLA films were prepared by casting 2 wt % dichloromethane solution onto a flat-bottomed glass Petri dish in a glass bell-type vessel and dried in atmospheric pressure at room

Table I. Time Dependence on Methanol and Ethanol Vapors on Permeability Through the PLA Film

	$P_{Methanol}\times10^{10}$ $\left[\frac{cm^3(STP)cm}{cm^2\cdot s\cdot cmHg}\right]$			$P_{Ethanol}\times10^{10}$ $\left[\frac{cm^3(STP)cm}{cm^2\cdot s\cdot cmHg}\right]$		
Time (min)	25°C	35°C	45°C	25°C	35°C	45°C
0-180	85.6 ± 3.56	342 ± 37.2	969 ± 10.8	<1	15.5 ± 1.4	86.0 ± 7.6
300	76.1 ± 14.4	183 ± 33.1	304 ± 34.8	<1	16.4 ± 2.4	46.9 ± 4.7
1000	93.9 ± 4.0	119 ± 20.5	173 ± 14.0	<1	14.9 ± 2.0	26.3 ± 3.6
1440	87.4 ± 22.8	109 ± 18.6	180 ± 15.8	<1	14.3 ± 1.7	26.0 ± 11.5

temperature. Each solvent was allowed to evaporate for 48 h. The dried PLA films were thermally treated in a vacuum for 48 h at 70°C to eliminate the residual solvent and to obtain amorphous PLA films. The thermally treated PLA films were then cooled at room temperature in atmospheric pressure. Proton nuclear magnetic resonance (^{1}H-NMR; NM-ECA500, JEOL Ltd., Tokyo, Japan) analysis results confirmed the removal of the residual solvent. The thickness of the films used in this study varied from 35 μm to 45 μm. The uncertainty for the thickness of each film was ± 1 μm.

Measurement of Permeation Properties of Pure Alcohol Vapor and Nitrogen

The permeation properties of pure single component (i.e., methanol, ethanol, and nitrogen) in PLA films were determined via the constant volume-variable pressure method at 25 ± 1°C, 35 ± 1°C, and 45 ± 1°C. The saturated vapor pressure (p_{sat}) values of methanol were 12.6, 20.9, and 33.3 cmHg for 25, 35, and 45°C, respectively, whereas the p_{sat} values of ethanol were 5.9, 10.3, and 17.3 cmHg for 25, 35, and 45°C, respectively.[9] The experiments were performed at relative feed pressure (p/p_{sat}) from 0.9 to 1.0 for 0 min to 1440 min. Nitrogen permeation was obtained at 76 ± 1 cmHg. The downstream pressure was maintained in a vacuum during the experiments. All permeation data were determined for at least three film samples to confirm the reproducibility of the experimental results. These samples were changed at each permeation time.

The permeability coefficient (P (cm^3(STP)cm/(cm^2 s cmHg))) was determined from eq. (1) according to literature.[8,10]

$$P=\frac{dp}{dt}\frac{273V}{760(273+T)}\frac{1}{A}\frac{1}{\Delta p}\ell \quad (1)$$

where dp/dt is the pressure increase in time (t) at steady state, V (cm^3) is the downstream volume, T (°C) is the temperature, A (cm^2) is the film area, Δp (cmHg) is the upstream pressure, and ℓ(cm) is the thickness of the film.

All characterization data were determined after alcohol vapor permeation in the range of 0 min to 1440 min. Moreover, the nitrogen permeation property was also determined after alcohol vapor permeation at each condition.

Film Characterization

All the characterization steps were performed using at least three samples of each film state after alcohol vapor exposure (permeation) to confirm the reproducibility of the experimental results. Fourier transform-infrared spectrometry (FT-IR) was carried out using the KBr method with FT/IR-4100 (JASCO Co., Tokyo, Japan) at 23 ± 1°C.

The film density (ρ) was determined using a density gradient column of aqueous calcium nitrate tetrahydrate (Junsei Chemical Co., Tokyo, Japan) solution with a density hydrometer at 23 ± 1°C.

Wide-angle X-ray diffraction (WAXD) measurements were performed using a Rint 1200 X-ray diffractometer (Rigaku Co. Ltd., Tokyo, Japan) with a Cu-Kα radiation source. The wavelength was 1.54 Å. Crystallinity (X_{C-WAXD}) was determined based on the percentage of the crystalline area in the maximum intensity peak.

The thermal analysis data were measured using a diamond differential scanning calorimeter (DSC; Perkin-Elmer Inc., Shelton). The sample pan-kit alum (Perkin-Elmer Inc., Shelton) was aluminum. Given that these data were used to discuss the gas transport properties, the first heating scan data (i.e., before annealing) represented the optimum condition relative to the second heating scan data. The heat scans were performed from 20 to 200°C at a heating rate of 10°C/min in nitrogen atmosphere. The glass transition temperature (T_g) was determined as the midpoint of the endothermic transition. The crystallization temperature (T_c) and the melting temperature (T_m) were determined as the maxima of each peak. Crystallinity ($X_{C\text{-}DSC}$) was estimated as follows:

$$X_{C\text{-}DSC}=\frac{\Delta H_m+\Delta H_c}{\Delta H_m^0}\times100 \quad (2)$$

where ΔH_m and ΔH_c are the melting and crystallization enthalpies of a polymer (J/g), respectively, and ΔH_m^0 is the enthalpy of the PLA (L-donor 100%) crystal, which has an infinite crystal thickness and a value of 93 J/g.[11]

Orthoscopic observation was conducted using an Olympus BX-51 polarization microscope (POM; Olympus Co., Tokyo, Japan) in a cross Nicol condition. Polarization images were observed under a colored additive at 530 nm by using a sensitive color plate.

Scanning electron microscopy (SEM) was performed using a high-resolution field scanning emission microscope (S5200, JEOL Ltd., Tokyo, Japan).

RESULTS AND DISCUSSION

Alcohol Vapor Permeability

Table I shows the methanol and ethanol vapor permeability coefficients of PLA films exposed to alcohol vapor at 25, 35, and 45°C. All PLA films used in this study were glassy at the

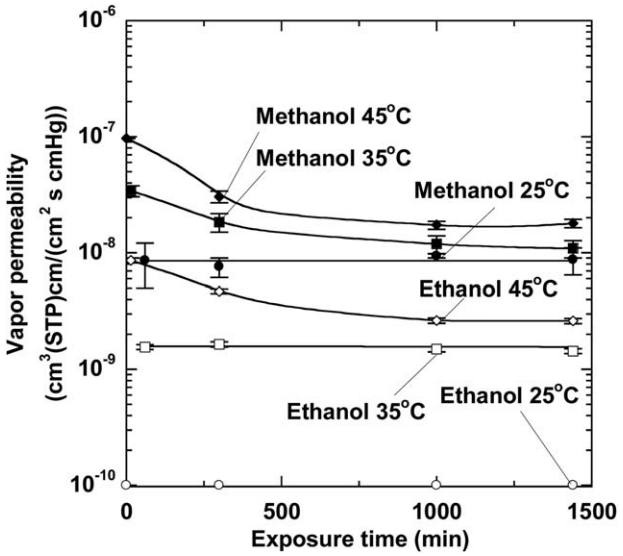

Figure 1. Time dependence of methanol and ethanol vapors on permeability through the PLA films. Temperature: 25°C (●), 35°C (■), and 45°C (◆) for methanol and 25°C (○), 35°C (□), and 45°C (◇) for ethanol.

experimental conditions. The lag time to reach the steady state was different from each condition in cohesive alcohol vapor. Therefore, the alcohol vapor permeability coefficient was assumed to be determined at the time where the steady state was reached (0–180 min). Figure 1 presents the alcohol vapor permeability coefficients of the PLA film at each temperature as functions of exposure (permeation) time.

The methanol vapor permeability clearly decreased in the exposure time range of 0 min to 300 min with increasing exposure time and gradually decreased to 1.80×10^{-8} cm^3(STP)cm/(cm^2 s cmHg) when the exposure time was increased from 300 min to 1440 min at 45°C. At 35°C, the permeability also clearly decreased in the exposure time range of 0 to 300 min and gradually decreased to 1.09×10^{-8} cm^3(STP)cm/(cm^2 s cmHg). This result is similar at 45°C. However, the permeability coefficients became constant in 7.61 to 9.39×10^{-9} cm^3(STP)cm/(cm^2 s cmHg) within the given time range at 25°C. The reduction in the methanol vapor permeability at a high temperature was more remarkable than at a low temperature.

On the other hand, the ethanol vapor permeability coefficient clearly decreased in the exposure time range of 0 to 300 min and gradually decreased to 2.60×10^{-9} cm^3(STP)cm/(cm^2 s cmHg) when the exposure time was increased from 300 to 1440 min at 45°C. In contrast to methanol vapor, the vapor permeability coefficient became constant within the range of 1.43 to 1.64×10^{-9} cm^3(STP)cm/(cm^2 s cmHg) at 35°C. The ethanol vapor permeability coefficient at 25°C could not be monitored for 1440 min. The ethanol vapor permeability coefficient was estimated to be below the order of 10^{-10} cm^3(STP)cm/(cm^2 s cmHg). The reduction in the ethanol and methanol vapor permeabilities at a high temperature was also more remarkable than that at a low temperature.

In general, a high-pressure cohesive penetrant, such as organic vapor, was shown to plasticize glassy polymer films. The plasticization phenomena involve several aspects in increasing the permeability coefficient, such as the time, pressure, and temperature dependence.[12] Over the last decade, the carbon dioxide permeability coefficient of 4,4-(hexafluoroisopropylidene) diphthalic anhydride 2,3,5,6-tetramethyl-1,4-phenylene diamine was reported to increase from 1.0×10^{-7} to 2.0×10^{-7} cm^3(STP)cm/(cm^2 s cmHg) at 3040 cmHg and 35°C for 12 h. However, these results indicate that the tendency showed the opposite behavior. Therefore, the structure of the PLA films after methanol and ethanol vapor permeation was systematically investigated to analyze the mechanism of decreasing vapor permeability.

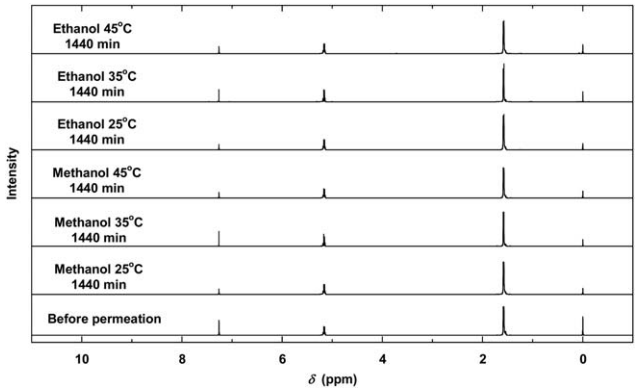

Figure 2. ^{1}H-NMR spectra of the PLA films exposed to methanol and ethanol vapors for 1440 min at 25, 35, and 45°C.

Film Characterization

The density of PLA films before alcohol vapor permeation was 1.257 g/cm^3, and the T_g value was 60.3°C. T_c and T_m peaks were not observed in the DSC thermograms. X_C values determined from DSC and WAXD were 0 %; thus, amorphous PLA films were used in this study.

Figures 2 and 3 show the ^{1}H-NMR and FT-IR spectra of the PLA films, respectively, exposed to alcohol vapor. PLA: ^{1}H-NMR; (500 MHz, $CDCl_3$-d, δ): 1.57–1.59 (3H, H^1), 5.10–5.19 (H, H^2); IR: 2960 and 2870 cm^{-1} (C−H stretching), 1750 cm^{-1} (C=O stretching), 1470 cm^{-1} (C−H stretching and C−H bending), 1180 and 1080 cm^{-1} (C–O–C). A difference in peak

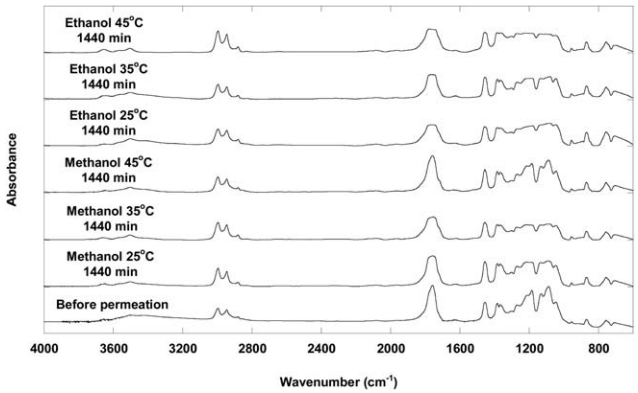

Figure 3. FT-IR spectra of the PLA films exposed to methanol and ethanol vapors for 1440 min at 25, 35, and 45°C.

Table II. Density of the PLA Films Exposed to Methanol and Ethanol Vapors

Solvent	Temperature (°C)	Time (min)	ρ (g/cm^3)
Unexposed[a]	-	0	1.257 ± 0.001
Methanol vapor	25	0–180	1.245 ± 0.001
		300	1.250 ± 0.001
		1000	1.259 ± 0.001
		1440	1.259 ± 0.001
	35	0–180	1.252 ± 0.001
		300	1.251 ± 0.001
		1000	1.252 ± 0.001
		1440	1.249 ± 0.002
	45	0–180	1.249 ± 0.001
		300	1.256 ± 0.001
		1000	1.257 ± 0.001
		1440	1.257 ± 0.001
Ethanol vapor	25	0–180	1.261 ± 0.001
		300	1.255 ± 0.002
		1000	1.259 ± 0.001
		1440	1.259 ± 0.001
	35	0-180	1.262 ± 0.001
		300	1.257 ± 0.001
		1000	1.256 ± 0.001
		1440	1.256 ± 0.002
	45	0–180	1.254 ± 0.008
		300	1.254 ± 0.001
		1000	1.255 ± 0.001
		1440	1.256 ± 0.001

[a] Data from Ref. 7.

position was not observed between the exposed and unexposed PLA films to alcohol vapor. This result indicates that no changes in chemical structure occurred during alcohol vapor exposure.

Table II lists the densities of the PLA films exposed to alcohol vapor. The densities of the PLA films exposed to methanol [Figure 4(a)] and ethanol [Figure 4(b)] as functions of exposure time are shown in Figure 4. The film density became constant within the given time. However, the densities of the PLA films exposed to methanol vapor at 35°C became slightly lower than those of the unexposed PLA film.

Figure 5 shows the photographs of the PLA films in this study. The transparent PLA films whose permeability was not changed were prepared by methanol vapor exposure at 25°C and ethanol vapor at 25 and 35°C, whereas the PLA films exposed to methanol vapor at 35 and 45°C and ethanol vapor at 45°C were slightly cloudy. These cloudy films are caused by crystallization for light diffusion, which was reported in our study.[3] The physical structures, including the crystalline structure, of the alcohol vapor-induced crystallized PLA films were systematically investigated.

Crystal Structure Analysis

X-ray Analysis. Figure 6 shows the WAXD patterns of the PLA films exposed to alcohol vapor. The vapor permeability coefficients of the PLA were unchanged, such as the PLA films exposed to methanol vapor at 25°C and ethanol vapor at 25 and 35°C, and only a broad peak was observed. By contrast, several sharp peaks near diffraction angles of 16.7° and 19.2° were observed in the PLA films, where the vapor permeability coefficients decreased, such as the PLA films exposed to methanol vapor at 35°C and 45°C and ethanol vapor at 45°C. The conditions for sample preparation of the PLA products significantly influenced their crystalline structures (α-, β-, and γ-form).[13] The Miller index of the α-form crystal diffraction peaks was observed at 16.7° and 19.2°, which is consistent with (200),

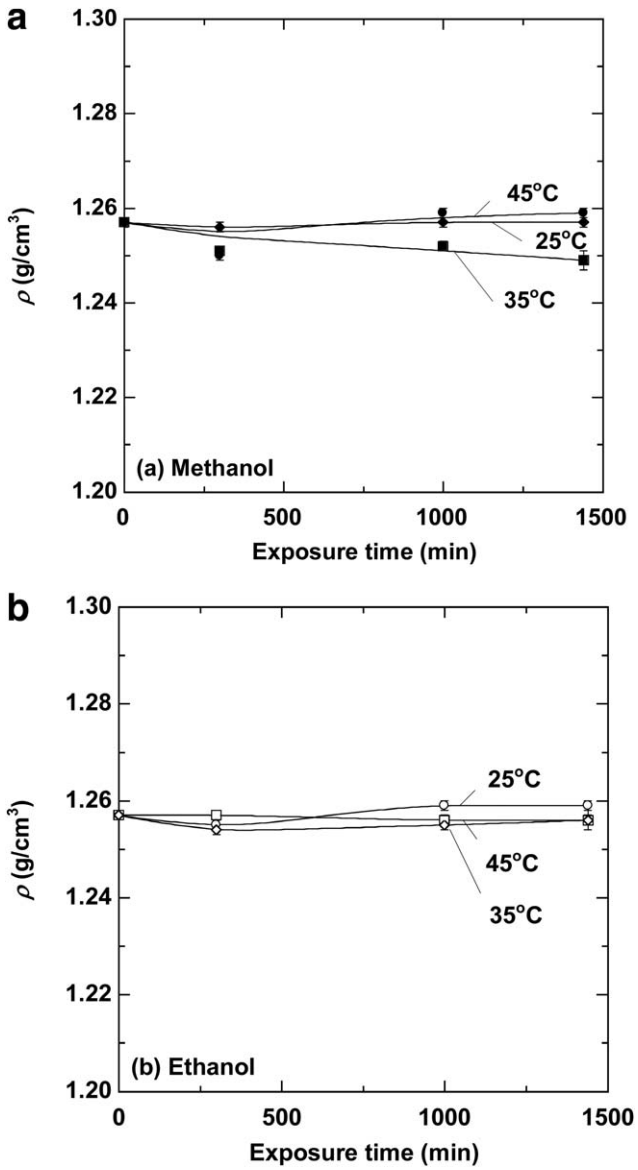

Figure 4. Film density as a function of exposure time in PLA the films exposed to (a) methanol and (b) ethanol vapors. Temperature: 25°C (●), 35°C (■), and 45°C (◆) for methanol and 25°C (○), 35°C (□), and 45°C (◇) for ethanol.

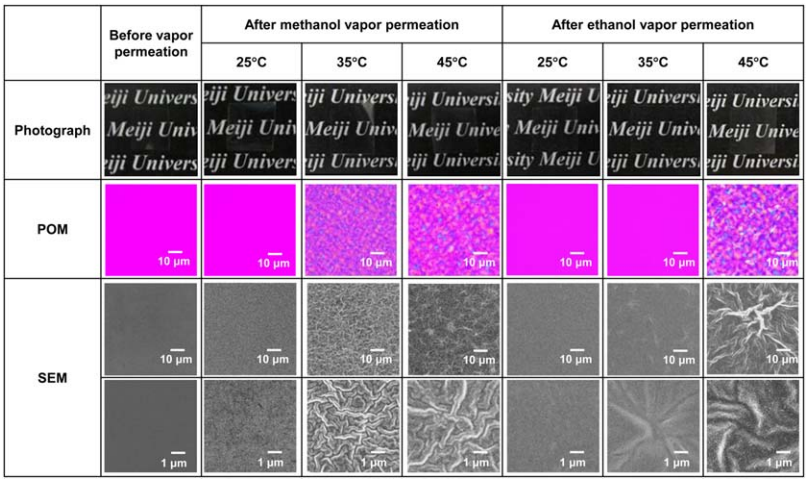

Figure 5. Photographs, POM, and SEM images of the PLA films exposed to methanol and ethanol vapors for 1440 min at 25, 35, and 45°C. [Color figure can be viewed in the online issue, which is available at wileyonlinelibrary.com.]

(110) and (100), (203), respectively.[14–16] The unit cell of the α-crystal structure has a space group of $P2_12_12_1$ and the following dimensions: a = 10.68 Å, b = 6.17 Å, c = 28.86 Å, and $\alpha = \beta = \gamma = 90°$.[17] The PLA films formed an α-crystal structure because their WAXD patterns clearly showed several sharp peaks at 16.7° and 19.2°.

Table III summarizes the $X_{C\text{-}WAXD}$ values determined using the WAXD patterns of the PLA films. The alcohol vapor-induced crystallized PLA film formed an α-crystal structure. In the PLA films whose vapor permeability coefficients decreased, such as the PLA films exposed to methanol vapor at 35 and 45°C and ethanol vapor at 45°C, the crystallinity significantly increased in

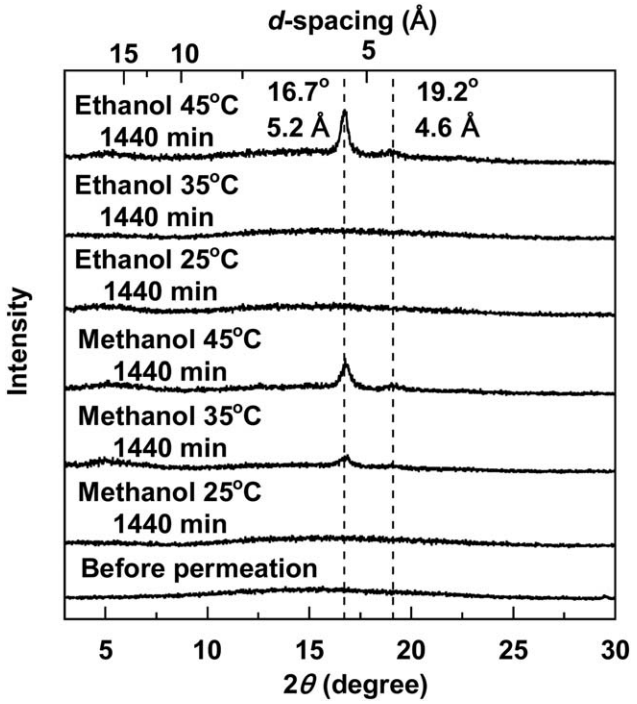

Figure 6. Wide-angle X-ray diffraction patterns of the PLA films exposed to methanol and ethanol vapors for 1440 min at 25, 35, and 45°C.

Table III. X-Ray Properties of the PLA Films Exposed to Methanol and Ethanol Vapors

Solvent	Temperature (°C)	Time (min)	$X_{C\text{-}WAXD}$ (%)
Unexposed[a]	-	0	0
Methanol vapor	25	0–180	0
		300	0
		1000	0
		1440	0
	35	0–180	0
		300	2.8 ± 0.7
		1000	10.4 ± 1.7
		1440	8.9 ± 1.1
	45	0–180	0
		300	9.9 ± 0.8
		1000	14.2 ± 1.4
		1440	17.9 ± 1.7
Methanol solvent[b]	35	1440	35.5 ±3.5
Ethanol vapor	25	0–180	0
		300	0
		1000	0
		1440	0
	35	0–180	0
		300	0
		1000	0
		1440	0
	45	0–180	0
		300	3.7 ± 2.0
		1000	12.4 ± 1.9
		1440	15.9 ± 1.4
Ethanol solvent[b]	35	1440	37.1 ±3.1

[a] Data from Ref. 7.
[b] Data from Ref. 3 at solvent.

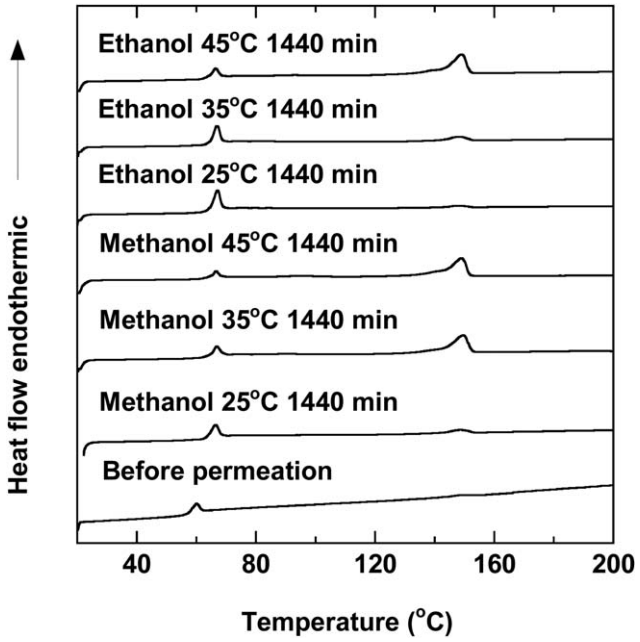

Figure 7. DSC thermograms of the first heating scan of the PLA films exposed to methanol and ethanol vapors for 1440 min at 25, 35, and 45°C.

the time range of 0 to 300 min and gradually increased in the time range of 300 to 1440 min. However, the crystallinity of the PLA films whose vapor permeability coefficients were unchanged could not be determined.

Thermal Analysis. Figure 7 shows the DSC thermograms of the PLA films exposed to alcohol vapor. The T_g, T_c, T_m, ΔH_c, and ΔH_m values determined using the DSC thermograms of the PLA films are summarized in Tables IV and V. Endothermic peaks were observed near 61.2 to 63.1°C in all PLA films used in this study. These peaks corresponded to T_g. The sample preparation conditions of the PLA products significantly influenced their thermal properties.[18] The literature data for PLA films showed a wide range of T_g values from 55 to 69°C.[5,18–24] The data obtained in this study were within the range of the literature values.

In the PLA films exposed to alcohol vapor, the peaks for crystallization and melting temperatures were observed. The literature value of T_c for PLA varied from 79 to 118°C.[5,18–24] Exothermic peaks were slightly observed near 107 to 117.9°C. The data of the alcohol vapor-exposed PLA film were within the range of the literature values. On the other hand, the literature values of T_m for PLA varied from 149 to 192°C.[5,18–24] The values of the alcohol vapor-exposed PLA film were 147.6 to 151.2°C. The data of the alcohol vapor-exposed PLA film were slightly lower than the literature values. The peaks for crystallization and melting temperatures were observed in the PLA films whose vapor permeability coefficients were unchanged, such as the PLA films exposed to methanol vapor at 25°C and ethanol vapor at 25 and 35°C. Alcohol vapor-induced crystallization was observed in all these PLA films.

Alcohol vapor-induced crystallization occurred in the PLA film through vapor permeation. Tables IV and V summarizes the X_{C-DSC} values of the methanol (Table IV) and ethanol (Table V) vapor-exposed PLA films, which were evaluated by eq. (2). The X_{C-DSC} values increased with increasing exposure time and temperature. Moreover, the increases in X_{C-DSC} of the PLA films whose vapor permeability coefficients were unchanged were more remarkable than those of the PLA films whose vapor permeability coefficients were changed. The X_{C-DSC} value of the methanol vapor-exposed PLA films was higher than that of the ethanol vapor-exposed PLA films. Moreover, as shown in Tables IV and V, the X_{C-DSC} values of the alcohol vapor-induced

Table IV. Thermal Properties of the PLA Films Exposed to Methanol Vapor

Temperature (°C)	Time (min)	T_g (°C)	T_c (°C)	T_m (°C)	ΔH_c (J/g)	ΔH_m (J/g)	X_{C-DSC} (%)
Unexposed[a]	0	60.3 ± 2.1	-	-	-	-	0.0
25	0-180	62.6 ± 0.2	117.9 ± 0.1	148.5 ± 0.1	−0.1 ± 0.1	1.7 ± 0.1	1.8 ± 0.1
	300	62.2 ± 0.2	117.9 ± 0.1	148.0 ± 0.5	−0.1 ± 0.1	2.0 ± 0.3	2.1 ± 0.3
	1000	62.8 ± 0.1	117.9 ± 0.1	148.5 ± 0.2	−0.1 ± 0.1	2.9 ± 0.4	3.0 ± 0.4
	1440	63.2 ± 0.3	119.0 ± 1.5	148.9 ± 0.5	−0.1 ± 0.1	2.6 ± 0.1	2.7 ± 0.1
35	0-180	62.5 ± 0.7	116.0± 2.7	148.6 ± 0.1	−0.2 ± 0.1	2.7 ± 0.7	2.8 ± 0.8
	300	63.1 ± 0.2	116.0 ± 0.4	148.8 ± 0.1	−0.9 ± 0.1	9.3 ± 0.2	9.0 ± 0.1
	1000	62.1 ± 0.6	110.0 ± 1.2	149.1 ± 0.4	−1.5 ± 0.6	15.5 ± 1.8	15.1 ± 1.3
	1440	62.7 ± 0.4	107.0 ± 3.1	149.0 ± 0.1	−1.5 ± 0.1	13.7 ± 0.1	13.1 ± 0.2
45	0-180	61.5 ± 1.4	117.5 ± 0.1	148.1 ± 0.3	−0.4 ± 0.1	4.2 ± 0.4	4.1 ± 0.5
	300	61.3 ± 2.0	112.7 ± 0.5	151.2 ± 3.6	−1.2 ± 0.1	15.2 ±0.1	15.0 ±0.1
	1000	61.2 ± 0.6	113.0 ± 0.6	149.0 ± 0.1	−0.9 ± 0.2	17.7 ± 0.3	18.0 ± 0.1
	1440	62.4 ± 0.1	112.5 ± 4.0	149.1 ± 0.1	−1.9 ± 0.2	16.4 ± 3.2	15.6 ± 3.3
35 (solvent)[b]	1000	53.0 ± 0.1	106.5 ± 0.3	144.6 ± 0.8, 149.3 ± 0.2.	−0.1 ± 0.1	23.1 ± 0.2	24.7 ± 0.1

[a] Data from Ref. 7.
[b] Data from Ref. 3 at solvent.

Table V. Thermal Properties of the PLA Films Exposed to Ethanol Vapor

Temperature (°C)	Time (min)	T_g (°C)	T_c (°C)	T_m (°C)	ΔH_c (J/g)	ΔH_m (J/g)	$X_{c\text{-}DSC}$ (%)
Unexposed[a]	0	60.3 ± 2.1	-	-	-	-	0.0
25	0-180	65.7 ± 0.3	117.8 ± 0.3	148.5 ± 0.5	−0.1 ± 0.1	1.9 ± 0.3	2.0 ± 0.3
	300	62.4 ± 4.4	115.9 ± 2.4	147.6 ± 0.3	−0.6 ± 0.3	4.1 ± 1.7	3.7 ± 1.5
	1000	63.4 ± 0.2	117.9 ± 0.1	149.0 ± 0.2	−0.2 ± 0.1	3.3 ± 0.2	3.4 ± 0.1
	1440	63.7 ± 0.3	118.1 ± 0.4	146.9 ± 0.6	−0.2 ± 0.2	1.3 ± 0.1	1.2 ± 0.2
35	0-180	63.9 ± 1.4	117.9 ± 0.1	148.5 ± 0.1	−0.1 ±0.1	3.1 ± 0.2	3.2 ± 0.2
	300	63.2 ± 0.8	117.6 ± 0.3	148.3 ± 0.7	−0.1 ± 0.1	2.0 ± 0.5	2.1 ± 0.4
	1000	62.8 ± 0.1	117.1 ± 0.4	147.8 ± 0.1	−0.4 ± 0.1	4.3 ± 1.1	4.1 ± 1.3
	1440	63.8 ± 0.3	117.4 ± 0.1	148.4 ± 0.6	−0.3 ± 0.1	3.4 ± 0.2	3.4 ± 0.3
45	0-180	63.0 ± 0.3	117.3 ± 0.6	148.4 ± 0.4	−0.1 ± 0.1	3.1 ± 0.4	3.2 ± 0.4
	300	62.4 ± 0.4	113.6± 0.8	148.4 ± 0.1	−1.3 ± 0.6	11.5 ± 4.3	10.9 ± 4.0
	1000	63.2 ± 0.3	109.3 ± 0.9	149.2 ± 0.5	−1.6 ± 0.1	17.2 ± 0.1	16.8 ± 0.1
	1440	62.8 ± 0.3	108.4 ± 0.4	149.0 ± 0.1	−1.5 ± 0.2	15.2 ± 0.3	14.8 ± 0.1
35 (solvent)[b]	1000	54.3 ± 1.0	101.9 ± 1.1	144.0 ± 0.6, 149.6 ± 0.5.	−0.4 ± 0.2	25.2 ± 0.9	26.7 ± 0.7

[a] Data from Ref. 7.
[b] Data from Ref. 3 at solvent.

crystallization was lower than that of alcohol solvent-induced crystallization, as shown in our previous study similar to the $X_{C\text{-}WAXD}$.[3]

Tables III to V clearly show that the $X_{C\text{-}WAXD}$ value was different from the X_{C-DSC} value. The $X_{C\text{-}WAXD}$ value was calculated using the peak fitting method, whereas the X_{C-DSC} value was directly determined through the enthalpy change. Therefore, the X_{C-DSC} value had a higher accuracy compared with the $X_{C\text{-}WAXD}$ value.

Microscope Analysis. Figure 5 presents the POM images of the alcohol vapor-exposed PLA films. POM images are the standard of dispersion of crystal domains. The PLA films exposed to methanol vapor at 25°C and ethanol vapor at 25 and 35°C showed an amorphous structure similar to the unexposed PLA film. However, the PLA films whose vapor permeability coefficients decreased, such as the PLA films exposed to methanol vapor at 35 and 45°C and ethanol vapor at 45°C, had dispersed blue color variation domains. The maximum size of one unit of color variation domains was 2 to 4 μm. Based on our previous study, the alcohol vapor-induced crystallization was similar to alcohol solvent-induced crystallization because of these configurations, including size and shape.

Figure 5 presents the SEM images of these alcohol vapor-exposed PLA films. The unexposed PLA films exhibited a smooth surface, whereas the PLA films exposed to alcohol vapors showed changes in surface structure. Crystal growth gradually branched out in a radial fashion in the alcohol vapor-exposed PLA films with increasing crystallinity. This invisible crystal morphologies depend on the cloudy films because light does not pass through the film.

Effects of Alcohol-Induced Crystallization on Vapor and Nitrogen Permeability

Alcohol vapor-induced crystallization behavior via the interaction with alcohol molecule through their vapor permeation was observed in the PLA film used in this study. Figure 1 shows that the reduction in the vapor permeability coefficients depends on crystallization because vapor molecules cannot diffuse and dissolve in the crystalline domain similar to other crystalline polymer films.

Figure 8 presents the alcohol vapor permeability coefficients of the PLA films as a function of crystallinity (X_{C-DSC}). A linear relationship between vapor permeability coefficients and X_{C-DSC} was observed. The vapor permeability decreased with increasing crystallinity. For PLA films, alcohol vapor is assumed to be

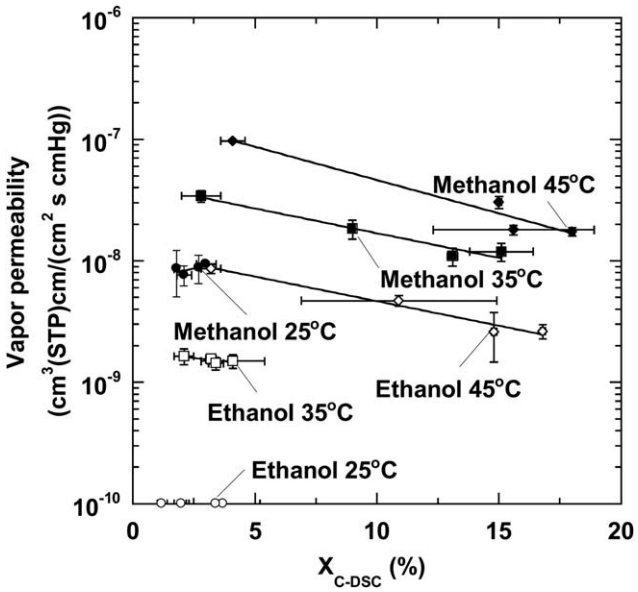

Figure 8. Effects of crystallinity on alcohol vapor permeability in the PLA films. Temperature: 25°C (●), 35°C (■), 45°C (◆) for methanol and 25°C (○), 35°C (□), and 45°C (◇) for ethanol.

Table VI. Time Dependence of PLA Film on Nitrogen Permeability After Methanol and Ethanol Vapor Permeation

	$P\times10^{12}\left[\frac{cm^3(STP)cm}{cm^2\cdot s\cdot cmHg}\right]$			$P\times10^{12}\left[\frac{cm^3(STP)cm}{cm^2\cdot s\cdot cmHg}\right]$		
	After methanol permeation			After ethanol permeation		
Time (min)	25°C	35°C	45°C	25°C	35°C	45°C
Unexposed	3.65 ± 0.54	5.04 ± 0.22[a]	7.51 ± 0.33	3.65 ± 0.54	5.04 ± 0.22[a]	7.51 ± 0.33
0–180	5.84 ± 0.23	6.63 ± 0.01	6.46 ± 0.03	3.98 ± 0.13	7.77 ± 0.14	6.98 ± 0.13
300	6.61 ± 0.04	8.24 ± 0.21	7.36 ± 0.33	6.55 ± 0.11	6.98 ± 0.27	6.96 ± 0.05
1000	5.67 ± 0.05	6.75 ± 0.39	8.09 ± 0.17	7.56 ± 0.02	6.37 ± 0.20	8.15 ± 0.26
1440	7.09 ± 0.37	6.57 ± 0.83	8.48 ± 0.02	7.93 ± 0.03	6.68 ± 0.33	6.34 ± 0.10

[a] Data from Ref. 7.

unable to permeate in the crystalline domain because alcohol vapor permeability depends on crystallinity.

On the other hand, the nitrogen permeability coefficients of the PLA films after alcohol vapor permeation at each temperature and time are shown in Table VI. The nitrogen permeability coefficients before and after methanol and ethanol vapor permeation at 45°C became constant from 6.46 × 10^{-12} to 8.48 × 10^{-12} cm^3(STP)cm/(cm^2 s cmHg). At 35°C, the nitrogen permeability coefficients before methanol and ethanol vapor permeation were 5.04 × 10^{-12} cm^3(STP)cm/(cm^2 s cmHg), whereas the permeability coefficients after permeation slightly increased from 6.37 × 10^{-12} to 8.24 × 10^{-12} cm^3(STP)cm/(cm^2 s cmHg). At 25°C, the nitrogen permeability coefficients before methanol and ethanol vapor permeation were 3.65 × 10^{-12} cm^3(STP)cm/(cm^2 s cmHg), whereas the permeability coefficients after permeation increased from 3.98 × 10^{-12} to

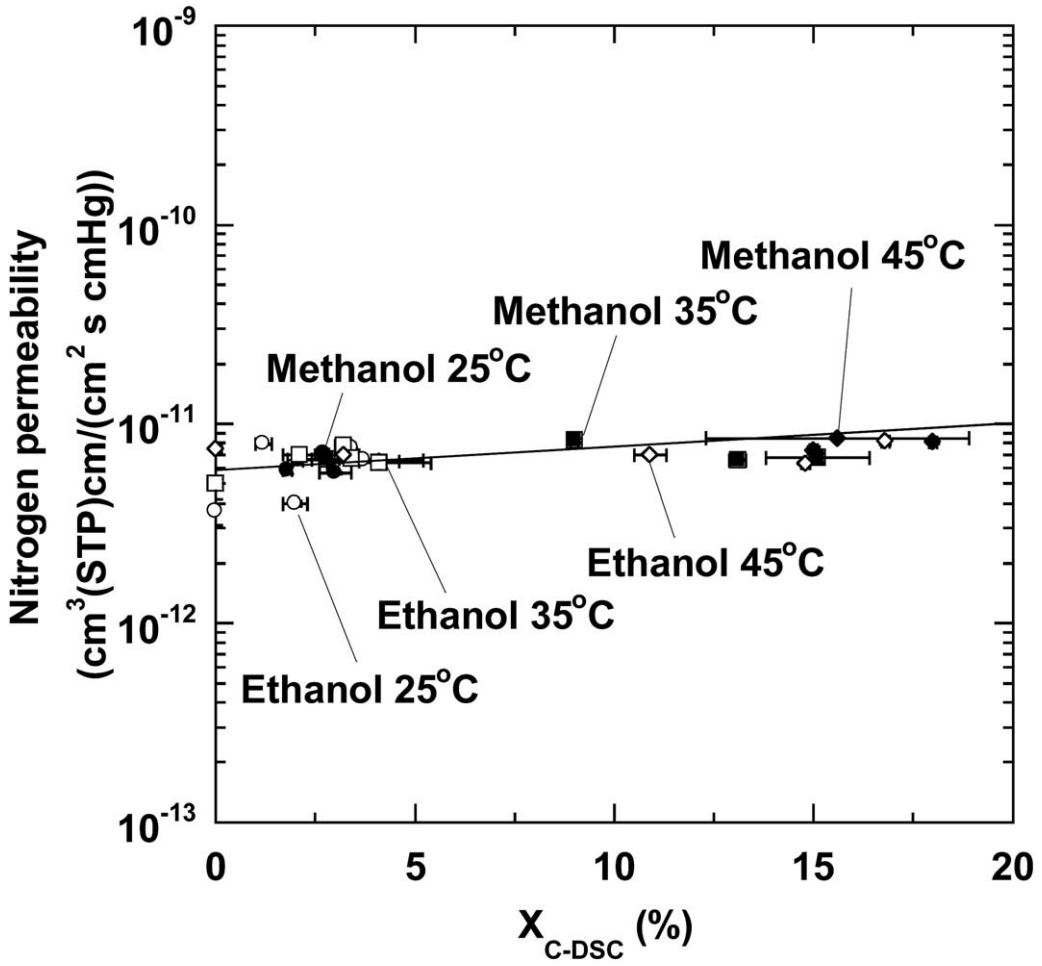

Figure 9. Effects of crystallinity on nitrogen permeability in the PLA films. Temperature: 25°C (●), 35°C ((■), 45°C ((◆) for methanol and 25°C (○), 35°C (□), and 45°C (◇) for ethanol.

7.93×10^{-12} cm^3(STP)cm/(cm^2 s cmHg). Figure 9 presents the nitrogen permeability coefficients of the PLA films after vapor permeation at each condition as functions of crystallinity (X_{C-DSC}). Interestingly, no linear relationship was observed between nitrogen permeability and crystallinity as opposed to alcohol vapor permeability. The nitrogen permeability tendency of the alcohol vapor-induced crystallized PLA films was the same as that of thermally induced crystallized PLA films in our previous study.[7] The decrease in permeability with increasing crystallinity was observed in alcohol vapor only.

As a result of DSC analysis, all PLA films exposed to alcohol vapor has crystalline structure. However, the permeability of PLA films was changed after contact with methanol vapor only at 35°C and 45°C and with ethanol vapor only at 45°C. The crystallinity of these PLA films was more than 9%. The alcohol vapor permeability of the PLA films whose crystallinity was less than 9% became constant. In this crystallinity range, the PLA films had a microphase separated structure between amorphous and crystalline regions based on POM and SEM analyses. The small space around the interface between crystalline and amorphous regions depended on the permeability, because those film densities were approximately constant in all experimental conditions, despite the changes of the PLA structure. The small continuous space around the interface enables gas to diffuse. The non-cohesive nitrogen permeability of the PLA films with large crystalline domain was higher than prior to crystallization because nitrogen molecules diffused in the bypass interface. On the other hand, in the case of cohesive alcohol vapors, the vapor permeability of the PLA films decreased in the high temperature condition. This is because the alcohol vapor was strongly introduced to the PLA film for vapor-induced crystallization in the high temperature. However, the nitrogen and alcohol vapor permeability of PLA films, whose crystalline domain was too small to analyze by microscopes, were not changed. The dependence of crystallinity on permeability was different from each penetrant. Moreover, total crystalline structures, including continuous crystal structures, remaining amorphous regions, and their interface also depend on vapor and gas permeabilities.

CONCLUSIONS

The effects of alcohol-induced crystallization on alcohol vapor permeability and their structures of PLA films were systematically investigated. The vapor permeability of the PLA films exposed to methanol vapor at 25°C and ethanol vapor at 25 and 35°C became constant with increasing exposure time. However, the PLA films exposed to methanol vapor at 35 and 45°C and ethanol vapor at 45°C decreased with increasing exposure time. The PLA films exposed to alcohol vapor became slightly cloudy, and no changes in chemical structure were observed. Alcohol vapor-induced crystallization was observed. The densities of the vapor-induced crystalline films were approximately similar to those of the amorphous film. The PLA films of the vapor-induced crystallization formed an α-crystal structure. The vapor permeability decreased with increasing crystallinity. However, the nitrogen permeability after vapor-induced crystallization was slightly higher than prior to crystallization. Total crystalline structures, including continuous crystal structures, remaining amorphous regions, and their interface also depend on vapor and gas permeabilities.

REFERENCES

1. Auras, R.; Harte, B.; Selke, S. *J. Sci. Food. Agric.* **2006**, *86*, 648.
2. Colomines, G.; Ducruet, V.; Courgneau, C.; Guinault, A.; Domenek, S. *Polym. Int.* **2010**, *59*, 818.
3. Sato, S.; Gondo, D.; Wada, T.; Kanehashi, S.; Nagai, K. *J. Appl. Polym. Sci.* **2013**, *129*, 1607.
4. Bao, L.; Dorgan, J. R.; Knauss, D.; Hait, S.; Oliveira, N. S.; Maruccho, I. M. *J. Membr. Sci.* **2006**, *285*, 166.
5. Komatsuka, T.; Kusakabe, A.; Nagai, K. *Desalination* **2008**, *234*, 212.
6. Paul, D. R.; Yampolskii, Y. P. Polymeric Gas Separtion Membranes; CRC Press: Boca Raton: FL, **1994**.
7. Sawada, H.; Takahashi, Y.; Miyata, S.; Kanehashi, S.; Sato, S.; Nagai, K., *Trans. Mater. Res. Soc. Jpn.* **2010**, *35*, 241.
8. Sato, S.; Ono, M.; Yamauchi, J.; Kanehashi, S.; Ito, H.; Matsumoto, S.; Iwai, Y.; Matsumoto, H.; Nagai, K. *Desalination* **2012**, *287*, 290.
9. Poling, B. E. The Properties of Gases and Liquids; McGraw-Hill: New York, **2001**.
10. Sato, S.; Suzuki, M.; Kanehashi, S.; Nagai, K. *J. Membr. Sci.* **2010**, *360*, 352.
11. Fischer, E. W.; Sterzel, H. J.; Wegner, G. *Kolloid Z. Z. Polym.* **1973**, *251*, 980.
12. Kanehashi, S.; Nakagawa, T.; Nagai, K.; Duthie, X.; Kentish, S.; Stevens, G. *J. Membr. Sci.* **2007**, *298*, 147.
13. Yasuniwa, M.; Tsubakihara, S.; Iura, K.; Ono, Y.; Dan, Y.; Takahashi, K. *Polymer* **2006**, *47*, 7554.
14. Pan, P.; Zhu, B.; Kai, W.; Dong, T.; Inoue, Y. *J. Appl. Polym. Sci.* **2008**, *107*, 54.
15. Wang, Y. M.; Funari, S. S.; Mano, J. F. *Macromol. Chem. Phys.* **2006**, *207*, 1262.
16. Zhang, J. M.; Duan, Y. X.; Sato, H.; Tsuji, H.; Noda, I.; Yan, S.; Ozaki, Y. *Macromolecules* **2005**, *38*, 8012.
17. Sasaki, S.; Asakura, T. *Macromolecules* **2003**, *36*, 8385.
18. Weir, N. A.; Buchanan, F. J.; Orr, J. F.; Farrar, D. F.; Boyd, A. *Biomaterials* **2004**, *25*, 3939.
19. Chen, C. C.; Chueh, J. Y.; Tseng, H.; Huang, H. M.; Lee, S. Y. *Biomaterials* **2003**, *24*, 1167.
20. Duek, E. A. R.; Zavaglia, C. A. C.; Belangero, W. D. *Polymer* **1999**, *40*, 6465.
21. Lee, J. H.; Park, T. G.; Park, H. S.; Lee, D. S.; Lee, Y. K.; Yoon, S. C.; Nam, J. D. *Biomaterials* **2003**, *24*, 2773.
22. Sarazin, P.; Roy, X.; Favis, B. D. *Biomaterials* **2004**, *25*, 5965.
23. Tsuji, H.; Suzuyoshi, K. *Polym. Degrad. Stab.* **2002**, *75*, 347.
24. Yao, F. L.; Bai, Y.; Chen, W.; An, X. Y.; Yao, K. D.; Sun, P. C.; Lin, H. *Eur. Polym. J.* **2004**, *40*, 1895.